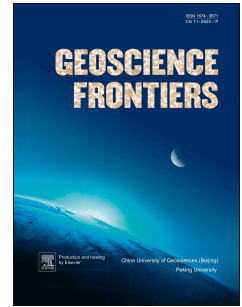


Accepted Manuscript

Payenia Quaternary flood basalts (Southern Mendoza, Argentina): Geophysical constraints on their volume

Mauro G. Spagnuolo, Darío L. Orts, Mario Gimenez, Andres Folguera, Victor A. Ramos



PII: S1674-9871(15)00122-X

DOI: [10.1016/j.gsf.2015.10.004](https://doi.org/10.1016/j.gsf.2015.10.004)

Reference: GSF 399

To appear in: *Geoscience Frontiers*

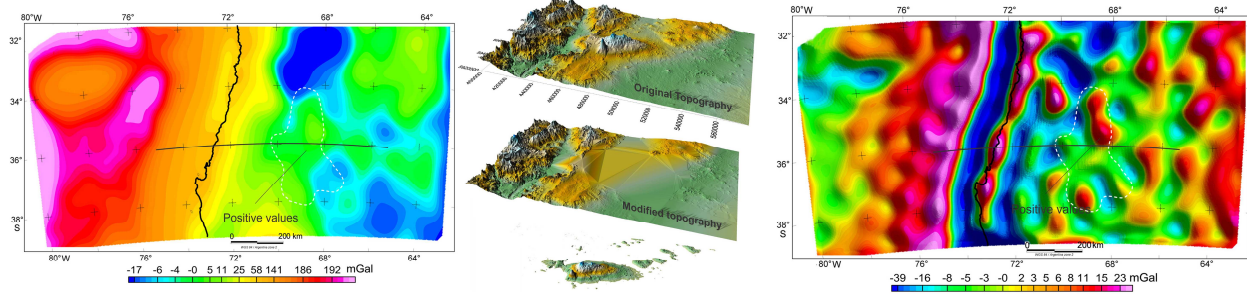
Received Date: 24 February 2015

Revised Date: 7 September 2015

Accepted Date: 6 October 2015

Please cite this article as: Spagnuolo, M.G., Orts, D.L., Gimenez, M., Folguera, A., Ramos, V.A., Payenia Quaternary flood basalts (Southern Mendoza, Argentina): Geophysical constraints on their volume, *Geoscience Frontiers* (2015), doi: 10.1016/j.gsf.2015.10.004.

This is a PDF file of an unedited manuscript that has been accepted for publication. As a service to our customers we are providing this early version of the manuscript. The manuscript will undergo copyediting, typesetting, and review of the resulting proof before it is published in its final form. Please note that during the production process errors may be discovered which could affect the content, and all legal disclaimers that apply to the journal pertain.



ACCEPTED MANUSCRIPT

1 Payenia Quaternary flood basalts (Southern Mendoza, 2 Argentina): Geophysical constraints on their volume

3
4 **Mauro G. Spagnuolo^{a,*}, Darío L. Orts^b, Mario Gimenez^c, Andres Folguera^a, Victor
5 A. Ramos^a**

6 ^a *Instituto de Estudios Andinos Don Pablo Groeber (I DEAN), UBA-CONICET*

7 ^b *Instituto de Investigación en Paleobiología y Geología, Universidad Nacional de Río
8 Negro – CONICET*

9 ^c *Instituto Geofísico y Sismológico Ing. Volponi, Universidad Nacional de San Juan.
10 CONICET*

11
12 *Corresponding Author: Intendente Güiraldes 2160. Ciudad Universitaria - Pabellón II.
13 C1428EGA – CABA, Argentina*

14 *Tel. (+54 +11) 4576-3400*

15 *E-mail address: mgsPag@gmail.com (Mauro G. Spagnuolo)*

26 **Abstract**

27 The Quaternary volcanic province of Payenia is located in southern Mendoza
28 and northern Neuquén provinces of Argentina and is characterized by a dominant
29 basaltic composition. The volcanic province covers an area larger than 40,000 km² and
30 its origin and evolution has been the center of several studies. In this study we analyzed

31 gravity data together with more accurate volcanic volumes calculations in order to
32 investigate the subsurface structure of the Payenia volcanic province. The volume of
33 material was calculated using digital elevation models and geographic information
34 system (GIS) techniques to estimate the volume of material erupted and then, with
35 those values, make an estimation of the intrusive material that could be located within
36 the crust. The results of the calculations were compared with different 2D-sections
37 constructed to model the gravity data and compare with the observed satellite gravity.
38 After evaluating different models which have been generated to match both: the
39 observed gravity data and the subsurface material calculated, we discuss those that
40 best fit with observation. The results clearly indicate that the lithosphere is attenuated
41 below the region.

42

43 Keywords: Payenia; Gravimetric model; Plume; Uplift; Andes

44

45

46 **1. Introduction**

47 In this study we used two independent techniques to study the subsurface
48 structure of the Payenia volcanic province. We used geographic information system
49 (GIS) techniques for volume calculations and gravimetric modeling to obtain a
50 quantification of the volume of igneous material by each independent method and then
51 we combined those results. The Southern Volcanic Zone of the Andes has a Quaternary
52 basaltic province along the retroarc which has a unique tectonic setting. The presence
53 of Payenia, a large Quaternary volcanic province of basaltic composition in the foreland
54 region, behind the active volcanic arc is unique in the entire Andean chain from
55 Colombia to Tierra del Fuego (Fig. 1). This volcanic province erupted through more than
56 800 volcanic centers in the last ~2 Ma, is developed between 33°30' and 38° over more
57 than 40,000 km² parallel to the active volcanic arc of the Southern Volcanic Zone (Stern
58 et al., 2004).

59 The entire volcanic region of mostly basaltic magmas was grouped by Ramos
60 and Folguera (2011) into three genetically related segments: (1) the northern sector
61 between 33°30' and 35°S is characterized by monogenetic volcanoes and cinder cones

62 with ages of less than 1.2 Ma; (2) the central section ($\sim 35^\circ$ to $36^\circ 30'S$) dominated by
63 large volcanic centers, and the Cerro Nevado, Llanquanelo and Payún Matrú volcanic
64 fields, and represents the largest erupted volume of the area; and (3) the southern
65 sector ($\sim 36.5^\circ$ to $38^\circ S$), which is dominated by the Auca Mahuida and Tromen
66 volcanoes together with several minor centers like Cerro Morado, La Carne, Carrizo,
67 and Cerro Los Loros (Ramos and Folguera, 2011).

68 The three segments share similar volcanic histories which postdate a common
69 continuous basaltic plateau (erupted after 2 Ma) characterized by intraplate
70 geochemical signatures (Ramos and Kay, 2006). This initial event, which would have
71 developed from south to north, is the basement over which the later volcanic fields and
72 monogenetic centers were established from 1.5 to 0.005 Ma (Ramos and Folguera,
73 2011).

74 The focus of this study is to arrive to a plausible density model of the subsurface
75 structure of the Payenia volcanic province, based mainly on gravimetric studies
76 supported by estimations of the extrusive and intrusive material volume. The scope is to
77 reconcile the large volumes of volcanic rocks with possible subsurface material
78 emplaced in the crust and the geodynamic evolution of the area.

79 We start the study by analyzing the gravity data in section 2 and follow with the
80 volume calculations techniques to constrain the subsurface structure of the Payenia
81 volcanic province. In order to obtain a 2D density model of the central sector of the
82 Payenia, we determined a rough geometry from magnetotelluric information using the
83 subsurface data from Burd et al. (2008, 2014) because it is an independent method and
84 give ancillary information for the properties and densities of the materials. Then we
85 refined the profile to match the modeled gravity with the observed gravity values
86 obtained freely from the ICGEM (<http://icgem.gfz-potsdam.de/ICGEM/>). The observed
87 values were derived from the EGM-2008 model (Pavlis et al., 2008, 2012) which uses
88 complete spherical harmonics up to a degree and order of 2150 and contains additional
89 coefficients to reach the degree of 2190 and order 2159. Finally we quantified volcanic
90 volume erupted based on the topography and then we estimated the volume of
91 associated intrusive material with those extrusive rocks. These results of these
92 calculations helped to constrain the amount of material and density contrasts in the 2D-

93 sections used in the gravity modeling. The obtained section was then discussed within
94 the geodynamic context for the area since Cretaceous times, in which the Payenia
95 volcanic province developed.

96

97 **2. Modeling gravity anomalies**

98 **2.1. Gravity data**

99 Several geophysical studies have been done in order to understand the thermal
100 state across the Payenia region especially dedicated to infer the crustal thickness
101 associated with the geodynamical setting. From the very beginning it was observed that
102 the region of the Payenia was not isostatically compensated (Diez Rodríguez and
103 Introcaso, 1986). Assuming densities of 2.67 g/cm^3 for the topography above the sea
104 level, 2.9 g/cm^3 for the crust, and 3.2 g/cm^3 for the mantle, a simple relation can be
105 used to calculate the roots of a given topography using the Eq. (1)

$$106 \quad R = 6.675 \cdot h \quad (1)$$

107

108 where h is the topography and R is the thickness of the roots for each topographic point
109 (Introcaso, 1997). Using a digital elevation model (DEM) SRTM-30, (which was slightly
110 smoothed for the calculations) and assuming that all the crust is isostatically
111 compensated by the Airy hypothesis, the thickness of the crust was calculated from Eq.
112 (1) and adding a normal crust of 35 km to the root thicknesses. The calculation of the
113 crustal thickness and the Isostatic correction was done with the software Oasis Montaj.
114 This result was then compared with the observed gravity derived from the EGM-2008
115 model obtained from the ICGEM (International Centre for Global Earth Models)
116 (<http://icgem.gfz-potsdam.de/ICGEM/>) (Fig. 2). The subtraction of the isostatic
117 correction from the Bouguer anomaly, assuming a perfectly compensated model, should
118 yield a zero isostatic anomaly. As seen in Fig. 2, the topographic profile at 36°S is near
119 to be fully compensated, but there are local anomalies which indicate that another
120 geodynamic process, and/or density heterogeneities present within the crust, would be
121 affecting the gravity signal.

122 It is well known that the Bouguer anomaly contains the sum of gravimetric effects
123 of different sources and there are many techniques that allow a proper separation of

124 such effects. Techniques using different frequencies were applied to identify those
125 different sources, like the upward continuation technique and Butterworth filter
126 (Ancillary fig. 1) (e.g., Blakely, 1995).

127 In order to isolate the short wave-lengths anomalies, which mostly correspond to
128 upper crustal gravimetric effects, we have discounted long wave-length anomalies using
129 an upward continuation analyses. These types of analyses recomputed the gravimetric
130 field to an arbitrary height above the registration level. The difference between the
131 upward continuation computed and the measured Bouguer anomalies constitutes a
132 residual grid that reflects short wave-lengths gravimetric components that mostly
133 correspond to upper crustal density contrasts.

134 The Airy decompensated isostatic anomaly was obtained by doing an upward
135 continuation up to 35 km above the sea level (Fig. 3a), to eliminate the superficial
136 anomaly sources and short wavelengths. This grid which reflects the long-wave
137 anomalies was subtracted to the original isostatic anomaly to obtain the short wave-
138 length components (Cordell, 1985). The value chosen for the $h= 35$ km to generate the
139 upward continuation was based on regional estimated values of crustal thickness. The
140 final grid represents a residual isostatic anomaly associated with bodies emplaced in
141 the upper crust. The results show that the larger anomalies coincide with the main
142 volcanic edifices like Cerro Nevado and Auca Mahuida located in the NE and SW of the
143 Payenia province respectively (Fig. 1). Both centers are characterized by high gravity
144 values that could be associated either with the superficial volcanic edifices itself and/or
145 with subvolcanic bodies emplaced in the upper crust. However, in the central part of the
146 Payenia, where the Payún Matru is located, there are no high gravity values, indicating
147 that shallow high density bodies are not sources of important anomalies (Fig. 3b). On
148 the other hand, by analyzing the upward continuation itself over the central area, a
149 positive anomaly is observed. This implies a deep high density source. To verify this
150 hypothesis for the anomaly we applied a filtering technique called Butterworth Filter with
151 a cutoff of 300 km and filter order 8 (Blakely, 1995). This filter eliminates anomalies
152 higher than 300 km wave-length but in the filtered grid a central positive anomaly can be
153 still observed favoring the hypothesis of an anomaly source at depth (Ancillary Fig. 1).

154

155 **2.2. Model construction**

156 To identify the sources responsible of the observed gravimetric anomalies,
157 different models in 2-D cross sections were generated to simulate their gravimetric
158 response. The simulated gravity profile of each section was compare with the observed
159 gravity data in order to verify their validity. These models were constrained by the
160 magnetotelluric data from Burd et al. (2008, 2014) who presented a conductivity model
161 for the first 500 km depth at 36°30'S; geometries and depth derived from seismic and
162 magnetotelluric data (Gilbert et al., 2006; Tassara, 2006); passive seismic studies
163 performed by Yuan et al. (2006) at 39°S; and the works of Folguera et al. (2007) and
164 Ramos y Folguera (2011), which proposed an attenuation of the crust under the area of
165 the Payenia supported by seismic data, which also show subcrustal low velocity zones
166 (Wagner et al., 2005; Gilbert et al., 2006). Based on all these results we constrained the
167 geometry of the density bodies in the cross section from which we obtained a modeled
168 Bouguer anomaly with the Oasis Montaj software that could be directly compared with
169 the observed Bouguer anomaly derived from the EGM-2008.

170 Using these geometries, fixed by independent data, we were allowed to test
171 different densities based on the “geological standard model” (Table 1), available seismic
172 velocity model for the wells near the area of study and previous papers after Ruiz and
173 Introcaso (1999); Introcaso et al. (2000); Fromm et al. (2004); Gilbert et al. (2006);
174 Giménez et al. (2006, 2009); Tassara et al. (2007) and Burd et al. (2014) for thermal
175 conditions. We obtained, after different tests, two plausible 2D-density models where
176 the calculated gravity fits with observed gravity.

177 In the first model that we show (Fig. 4a) we reproduced the derived geometry
178 from seismic and magnetotelluric sections from Gilbert et al. (2006) and Burd et al.
179 (2008, 2014) assigning different densities depending on the composition and thermal
180 state of the material. The model includes a plume of hotter material, which is uprising
181 from the 660 km mantle discontinuity, potentially from stagnant subducted oceanic
182 slabs. This strong asthenospheric influx due to the steepening of the subducted Nazca
183 plate has been invoked to trigger the large amount of the Pliocene to Quaternary
184 retroarc volcanism of the Payenia (Bertotto et al., 2009; Folguera et al., 2009; Burd et
185 al., 2014; Ramos et al., 2014). We also included in the model, together with this plume

186 of hot material (Burd et al., 2014), an attenuated crust towards the foreland area below
187 Payenia province. The crustal attenuation in the model is in the order of 10 km. This
188 amount of crustal thinning is needed to match the modeled and observed gravity, and it
189 is in agreement with passive seismic data (Gilbert et al., 2006, Ramos and Folguera,
190 2011). This crustal attenuation could be inferred from the decompensated isostatic
191 anomaly map that indicates an excess of mass at depth where normal crustal material
192 would be replaced by dense mantle material.

193 Despite the gravimetric anomalies of the model from Fig. 4a match the observed
194 data, an alternative model was tested in which we incorporated a 13 km thick planar
195 body of dense subvolcanic material instead of the attenuation of the crust (Fig. 4b). Both
196 models are plausible, and have a similar gravimetric response, but to verify which of the
197 two models is more appropriate we estimated the amount of material that could have
198 been emplaced below as a function of the extruded material.

199
200

201 **2.3. Volcanic volume calculations**

202 To calculate the volume of volcanic material emplaced in the crust, we first made an
203 estimation of the eruptive volume, based on DEMs analyses. We used radar topography
204 from Shuttle Radar Topography Mission (SRTM) (Farr et al., 2007) and topographic
205 data from Advanced Spaceborne Thermal Emission and Reflection Radiometer data
206 (ASTER GDEM Version 1, Fujisada et al., 2005). The calculated eruptive volume is
207 based on the definition of two surfaces: a lower one represented by a mean base level,
208 and the upper one which is the present topography. This methodology proves to be
209 efficient for individual volcanoes (Völker et al., 2011). The volume calculations were
210 made in a sequential mode, based on the different ages of volcanism, starting by the
211 younger ones and continuing to subsequent older material. First we performed a
212 Geographic Information System (GIS) using the ages and maps compiled from Ramos
213 and Folguera (2011) together with the topography of the area. Later on we grouped the
214 material into three intervals based on the different ages (Table 2). The first interval
215 between the present and 0.6 Ma, the second one between 0.6 and 1.165 Ma, and the
216 third one between 1.165 and 2.5 Ma. These time lapses were based on three stages of

217 evolution of the Payenia volcanic field (Ramos and Folguera, 2005; Folguera et al.,
218 2008; Risso et al., 2008; Ramos and Folguera, 2011).

219 After defining the time intervals, we calculated the volume for the first one placing
220 the lower plane at the base of the volcanoes with ages younger than 0.6 Ma and for the
221 top surface we used the topography. After calculating the volume between these two
222 surfaces we cut the topographic grid, erasing any topography within that interval. Then
223 the grid was interpolated again to cover removed parts and we obtained a new
224 topographic grid without the younger material. The new grid was used as entry for the
225 subsequent interval calculations, as the top surface, placing a new lower plane at the
226 base of the 1.165 Ma old material and repeated the procedure. Finally, the total volume
227 calculated for the volcanic centers, adding the figures from the three intervals, is 1469
228 km³ (Table 2).

229 All these local centers stand above a basaltic plateau younger than ~2 Ma.
230 Llambías et al. (2010) mentioned that in the distal parts the plateau is between 6 and 20
231 m thick, constraining the minimum thickness value. The total area, including the basal
232 plateau, is ~40,660 km². Taking into account this measurement and the regional slope,
233 a conservative number for the thickness of this volcanic platform at the center of the
234 plateau could be between 150 and 200 m. Based on these values and the total area
235 measured from the DEM, the volume of the plateau is between 6100 and 8132 km³,
236 which together with the previous 1469 km³ measured for the individual volcanic centers,
237 results in a total volume between 7569 and 9601 km³. These figures are in agreement
238 with previous estimations of ~8400 km³ (Risso et al., 2008; Németh et al., 2011; Ramos
239 and Folguera, 2011).

240 With these results of the estimations of erupted volume, the next step was to
241 estimate the volume of intrusive material emplaced on the upper crust to compare this
242 result with the thickness of the subsurface material predicted by the gravity models (see
243 section 2.1). Studies of intrusive volcanism suggest a role for intrusive bodies as the
244 hidden component of the broader volcanic system that is expressed at the surface as
245 volcanism. A compilation of magma emplacement and volcanic output gives ratios of
246 intrusive to extrusive volumes in the ranges 5:1 for oceanic settings and 10:1 for
247 continental ones (Crisp, 1984). Others estimations for the relation between intrusive and

248 erupted volumes vary between 3:1 and 16:1 (Smith and Shaw, 1975, 1979; Crisp, 1984;
249 Francis and Hawkesworth, 1994; de Silva et al., 2007), being 3:1 and 5:1 the most
250 conservative ones (Crisp, 1984; White et al., 2006; de Silva et al., 2007). Despite these
251 rates between intrusive vs. extrusive material were not calculated for an exact similar
252 environment as the Payenia volcanism, we consider that are applicable and
253 conservative ones sincere present a broad stiles of volcanic settings.

254 Using these relations, we first estimated the volume of subsurface material and
255 then, divided that value by the area enclosed by the surface volcanism to obtain the
256 thickness of a possible tabular body emplaced under the surface (Table 3). In the next
257 section we discuss the relation between the thickness values for the subcrustal igneous
258 material obtained by the calculations, and the 2D density sections of the gravity
259 modeling.

260

261 **3. Conclusions**

262 In section 2.1 we discussed two possible density models to explain observed
263 gravity: one introducing a crustal thinning, and a second one without such a crustal
264 thinning but considering the emplacement of an important amount of mafic material
265 within the crust. This last model requires a large amount of material equivalent to a 13
266 km thick body to match the modeled gravity with the observed one. This thickness is
267 incompatible with the volume calculations made in section 2.3. We showed that with an
268 end member relation of intrusive-extrusive material rate of 16:1 the thickness of
269 subsurface material would be around 4 km which is a much lower value than the
270 required to match the gravity data if we only consider the presence of subsurface dense
271 material. This result shows that crustal thinning is crucial to explain the gravity values
272 and subsurface denser material by itself, can't explain the gravity data. Based on this
273 conclusion we finally present a model where we incorporated both: subsurface dense
274 material and crustal thinning (Fig. 6). In the 2-D section we incorporated a 4 km thick
275 denser body and then we adjust the base of the crust to match the observed gravity.
276 This model explains gravity observations and is compatible with the volcanic volume
277 calculations together with the intrusive material estimations. In this last model we also
278 incorporated the geometry of hotter material spots by Burd et al. (2014) instead of a

279 mean geometry defining a plume feature as shown in their previous work (Burd et al.,
280 2008, 2014). Moreover, the spectral analysis of magnetic anomalies allows evaluating
281 the depth to the Curie temperature (Bhattacharyya and Leu, 1975; Blakely, 1988, 1995;
282 Tanaka et al., 1999), which would be associated with changes in the vertical distribution
283 of temperatures in the crust (Zorin y Lepina, 1985; Ruiz and Introcaso, 2001). If in fact
284 the crustal thinning predict by the model of Fig. 6 exists then the magnetic anomalies
285 must show a similar scenario. Following Tanaka et al. (1999), and using the world
286 magnetic anomalies model WMM2010, Novara (2012) calculated the depth of the
287 isotherm of 573 °C for this region which is assumed to correspond to the Curie depth
288 point, and therefore the crustal thermal structure can be directly inferred from magnetic
289 data (Fig. 7). The Curie isotherm is shallower in the studied area towards the foreland,
290 indicating a higher heat flux under the Payenia and supporting the model from Fig. 6
291 that shows there is a crustal attenuation zone. Moreover, Søger et al. (2013)
292 demonstrated, based on geochemical analysis of the volcanic rocks from Payenia, that
293 extensive melting of lower crust occurred, and was probably related to the low thickness
294 of the lithospheric mantle and preheating of the lower crust by earlier Mio-Pliocene
295 volcanism. They also suggest a thinner lithosphere in the western Payenia region
296 compared to the eastern one (Søger et al., 2013), a characteristic that it is also seen in
297 Fig. 7. This crustal thinning episode could be related to an extensional setting that
298 postdated the slab shallowing episode of 18–4 Ma and would be related to a steepening
299 of the slab that favored the emplacement of hot material.

300

301

302

303

304 **Acknowledgments**

305 Dr. A. Burd and an anonymous are thanked for their critical comments that helped to
306 improve the manuscript. Thanks also go to the editors for improvement and help with
307 the language. This is the contribution R-174 of IDEAN.

308

309

310 **References**

311 Blakely, R.J., 1995. Potential Theory in Gravity and Magnetic Applications.
312 Cambridge University Press, Cambridge, 441 pp.

313

314 Burd, A. Booker, J.R., Mackie, R., Favetto, A., Pomposiello, M.C., 2014. Three-
315 dimensional electrical conductivity in the mantle beneath the Payún Matrú Volcanic
316 Field in the Andean backarc of Argentina near 36.5°S: evidence for decapitation of a
317 mantle plume by resurgent upper mantle shear during slab steepening. *Geophysical*
318 *Journal International* 198 (2), 812-827. doi:10.1093/gji/ggu145.

319

320 Burd, A. Booker, J.R., Pomposiello, M.C., Favetto, A., Larsen, J., Giordanengo,
321 G. and Orozco Bernal, L., 2008. Electrical conductivity beneath the Payún Matrú
322 Volcanic Field in the Andean back-arc of Argentina near 36.5°S: Insights into the
323 magma source. 7th International Symposium on Andean Geodynamics (Nice),
324 Extended abstract, 90-93.

325

326 Cordell, L., 1985. Techniques, applications, and problems of analytical
327 continuation of New Mexico aeromagnetic data between arbitrary surfaces of very high
328 relief. *Proceedings of the International Meeting on Potential Fields in Rugged*
329 *Topography*, Institute of Geophysics, University of Lausanne, Bulletin 7, 96-99.

330

331 Crisp, J.A., 1984. Rates of magma emplacement and volcanic output. *Journal of*
332 *Volcanology and Geothermal Research* 20(3), 177–221.

333

334 de Silva, S.L. y Gosnold, W.D., 2007. Episodic construction of batholiths: Insights
335 from the spatiotemporal development of an ignimbrite flare-up. *Journal of Volcanology*
336 *and Geothermal Research* 167 (1), 320-335.

337

338 Díez Rodríguez, A. and Introcaso, A., 1986. Perfil transcontinental sudamericano
339 en el paralelo 39°S. *Geoacta* 13 (2), 179-281.

340

341 Folguera, A., Bottesi, G., Zapata T., Ramos, V.A. 2008. Crustal collapse in the
342 Andean back-arc since 2 Ma: Tremen volcanic plateau, Southern Central Andes
343 ($36^{\circ}40' - 37^{\circ}30'S$). *Tectonophysics (Special Issue Andean Geodynamics)* 459, 140-160.

344
345 Folguera, A., Introcaso, A., Giménez, M., Ruiz, F., Martinez, P., Tunstall, C.,
346 García Morabito, E., Ramos, V.A., 2007. Crustal attenuation in the Southern Andean
347 retroarc ($38^{\circ} - 39^{\circ}30' S$) determined from tectonic and gravimetric studies: The Lonco-
348 Luán asthenospheric anomaly. *Tectonophysics* 439, 129–147.

349
350 Fromm, R., Zandt, G., Beck, S.L., 2004. Crustal thickness beneath the Andes
351 and Sierras Pampeanas at $30^{\circ}S$ inferred from Pn apparent phase velocities.
352 *Geophysical Research Letters* 31, L06625.

353
354 Francis, P.W., Hawkesworth, C.J., 1994. Late Cenozoic rates of magmatic
355 activity in the Central Andes and their relationships to continental crust formation and
356 thickening. *Journal of the Geological Society* 151, 845–854.

357
358 Gilbert, H., Beck, S., Zandt, G., 2006. Lithospheric and upper mantle structure of
359 central Chile and Argentina. *Geophysical Journal International* 165, 383–398

360
361 Giménez, M.E., Martínez, M.P., Bustos, G., Jordan, T., Lince Klinger, F., Mallea,
362 M., Girardi Gallego Guardia, A., 2006. Evaluación del Movilismo Hidrostático del Valle
363 De La Rioja, La Rioja Argentina *Revista Ciencias - FCEF- UNSJ* 10 (1), 3–11.

364
365 Giménez, M.E., Martinez, M. P., Jordan, T., Ruiz, F., Lince Klinger, F., 2009.
366 Gravity characterization of the La Rioja Valley Basin, Argentina. *Geophysics* 74(3),
367 B83–B94.

368
369 Introcaso, A., 1997. *Gravimetría*. UNR Editora, Rosario. Argentina, 355 pp.

370

371 Introcaso, A., Pacino, M.P., Guspí, F., 2000. The Andes of Argentina and Chile:
372 Crustal configuration, Isostasy, Shortening and Tectonic features from Gravity Data.
373 Temas de Geociencia 5 UNR Editora.

374
375 Németh, K., Risso, C., Nullo, F., Kereszturi, G., 2011. The role of collapsing and
376 cone rafting on eruption style changes and final cone morphology: Los Morados scoria
377 cone, Mendoza, Argentina. *Central European Journal of Geosciences* 3 (2), 102-118.

378
379 Pavlis, N.K., Holmes, S.A., Kenyon, S.C. and Factor, J.K., 2008. An earth gravitational
380 model to degree 2160: EGM2008. Paper Presented at the 2008 General Assembly of
381 the European Geosciences Union, Vienna, Austria.

382
383 Pavlis, N.K., Holmes, S.A., Kenyon, S.C. and Factor, J.K., 2012. The development and
384 evaluation of the Earth Gravitational Model 2008. *Journal of Geophysical Research:*
385 *Solid Earth* 117 (4), B04406

386 Prezzi, Claudia B., Götze, H-J., Schmidt, S., 2009. 3D density model of the Central
387 Andes. *Physics of the Earth and Planetary Interiors* 177(3–4), 217–234.

388
389 Ramos, V. A. and Folguera, A., 2011. Payenia volcanic province in the Southern
390 Andes: An appraisal of an exceptional Quaternary tectonic setting. *Journal of*
391 *Volcanology and Geothermal Research* 201(1–4), 53-64. doi:
392 <http://dx.doi.org/10.1016/j.jvolgeores.2010.09.008>.

393
394 Ramos, V.A., Folguera, A., 2005. Tectonic evolution of the Andes of Neuquén:
395 Constraints derived from the magmatic arc and foreland deformation". In: Veiga, G.,
396 Spalletti, L., Howell J., Schwarz E. (Eds.), *The Neuquén Basin: A case study in*
397 *sequence stratigraphy and basin dynamics*. Geological Society, Special Publication,
398 London, 252p.

399
400 Ramos, V.A., Kay, S.M., 2006. Overview of the Tectonic Evolution of the
401 Southern Central Andes of Mendoza and Neuquén (35°– 39°S Latitude). In: Kay, S.M.,

402 Ramos, V.A. (Eds.), Evolution of an Andean margin: A tectonic and magmatic view from
403 the Andes to the Neuquén Basin (35°–39°S latitude). Geological Society of America,
404 Special Paper 407, 1-18.

405
406 Risso, C., Németh, K., Combina, A.M., Nullo, F., Drosina, M., 2008. The role of
407 phreatomagmatism in a Plio-Pleistocene high-density scoria cone field: Llancanelo
408 Volcanic Field (Mendoza), Argentina. *Journal of Volcanology and Geothermal Research*
409 169, 61–86.

410
411 Ruiz, F., Introcaso, A., 1999. Geophysical evidence of crustal ancient junction in
412 Desaguadero-Bermejo megafault (San Juan-La Rioja Province, Argentina). *Acta*
413 *Geodética et Geophysica Hungarica*. Sopron.

414
415 Ruiz, F., Introcaso, A., 2001. Profundidades al punto de Curie en la Precordillera
416 Cuyana obtenidas por análisis espectral de anomalías magnéticas. *Temas de*
417 *Geociencia* 8, UNR Editora, Rosario. 36 pp.,

418
419 Smith, R.L., Shaw, H.R., 1975. Igneous Related Geothermal Systems.
420 Assessment of Geothermal Resources of the United States — 1975. In: White, D.E,
421 Williams, D.L. (Eds.) *United States Geological Survey Circular* 726, 58–83.

422
423 Soager, N., Holm, P.M., Llambias, E.J., 2013. Payenia volcanic province,
424 southern Mendoza, Argentina. *Chemical Geology* 349, 36 - 53.

425
426 Tanaka, A., Obuko Y., Matsubayashi, O., 1999. Curie point depth based on
427 spectrum analysis of the magnetic anomaly data in East and Southeast Asia.
428 *Tectonophysics* 306, 461-470.

429
430 Tassara, A., 2006. Factors controlling the crustal density structure underneath
431 active continental margins with implications for their evolution. *Geochemistry,*
432 *Geophysics, Geosystems* 7 (1), Q01001.

433

434 Tassara, A. , Swain, C., Hackney, R., Kirby J., 2007. Elastic thickness structure
435 of South America estimated using wavelets and satellite-derived gravity data. *Earth and*
436 *Planetary Science Letters* 253, 17–36.

437

438 Völker, D., Kutterolf, S., Wehrmann, H., 2011. Comparative mass balance of
439 volcanic edifices at the southern volcanic zone of the Andes between 33°S and 46°S.
440 *Journal of Volcanology and Geothermal Research* 205 (3), 114-129.

441

442 Wagner, L. S. Beck, S., Zandt, G., 2005. Upper mantle structure in the south
443 central Chilean subduction zone (30° to 36°S). *Journal of Geophysical Research* 110,
444 B01308. doi:10.1029/2004JB003238.

445

446 White, S.M., Crisp, J.A., Spera, F.A., 2006. Long-term volumetric eruption rates
447 and magma budgets. *Geochemistry, Geophysics, Geosystems* 7, Q03010.
448 doi:10.1029/2005GC001002.

449

450 Yuan, X., Asch, G., Bataile, K., Bohm, M., Echtler, H., Kind, R., Onchen, O.,
451 Wölbern, I., 2006. Deep seismic images of the Southern Andes. In: Kay, S.M., Ramos,
452 V.A. (Eds.), *Late Cretaceous to Recent Magmatism and Tectonism of the Southern*
453 *Andean Margin at the Latitude of the Neuquen Basin (36–39°S)*. Geological Society of
454 America, Special Paper 407, 61–72 pp.

455

456 Zorin, Y.A., Lepina, S.V., 1985. Geothermal aspects of development of
457 asthenospheric upwellings beneath continental rift zones. *Journal of Geodynamics* 3, 1–
458 22.

459

460

461

462

463

464 **Figure captions**

465 Figure 1. (A–A') Location of the gravimetric profile modeled in this work. B–B'
466 magnetotelluric and seismic tomography profiles from Gilbert et al. (2006) and Burd et
467 al. (2008); dashed line represents the array from Burd et al. (2014). Inset shows the
468 three volcanic segments of the studied area and ages of the main volcanic centers
469 (Ramos and Folguera, 2011).

470
471 Figure 2. (a) Calculated Bouguer and isostatic Airy gravity anomalies based on
472 (b) estimated roots of the Andes at 36°S from a topographic profile and Eq. (1).

473
474 Figure 3. (a) Upward continuation to 35 km in altitude derived from model EGM-
475 2008 (Pavlis et al., 2008, 2012). Note that the area below the Payenia (white
476 dashed line) shows relative high gravity values. (b) Decompensated isostatic
477 anomaly that shows anomalies caused by shallow density contrasts. All positives
478 represent bodies with densities higher than 2.6 g/cm³

479
480 Figure 4. (a) Density model considering crustal attenuation below the Payenia
481 and (b) density model with a high density intracrustal material emplaced (dashed line
482 represents the modeled anomaly and full thin line the observed one).

483
484 Figure 5. Graphic sequence of the methodology used to compute the volcanic
485 eruptive volume. Color bar code represents topographic values in meters.

486
487 Figure 6. Final density model based on Burd et al. (2014) and estimations of
488 intracrustal high density material from this work (dashed line represents the modeled
489 anomaly while full thin line the observed one).

490
491 Figure 7. Map showing the depth to the Curie isotherm. Payenia flood basalts
492 province is enclosed in a black full line and modeled profile discussed in the text in
493 dashed line. The Curie isotherms show a crustal attenuation zone to the east of the
494 profile in agreement with the gravity models.

495

496 **Table headings**

497 Table 1 Used densities in the 2-d sections (Giménez et al., 2006, 2009).

498

499 Table 2 Volcanic volume calculated based on the topography and the age
500 intervals.

501

502 Table 3 Results of the extrusive vs. intrusive volumes of volcanic material.

Table 1 Used densities in the 2-d sections (Giménez et al., 2006, 2009).

Parameters	Values
Topographic density above sea level	2.67 g/cm ³
Sediments average density	2.3 g/cm ³
Top crust density	2.7 g/cm ³
Lower crust density	2.9 g/cm ³
Lithosphere mantle density	3.2 g/cm ³
Asthenospheric material density	2.9 g/cm ³
Oceanic slab density	3.15 g/cm ³
Crust normal thickness	35 km

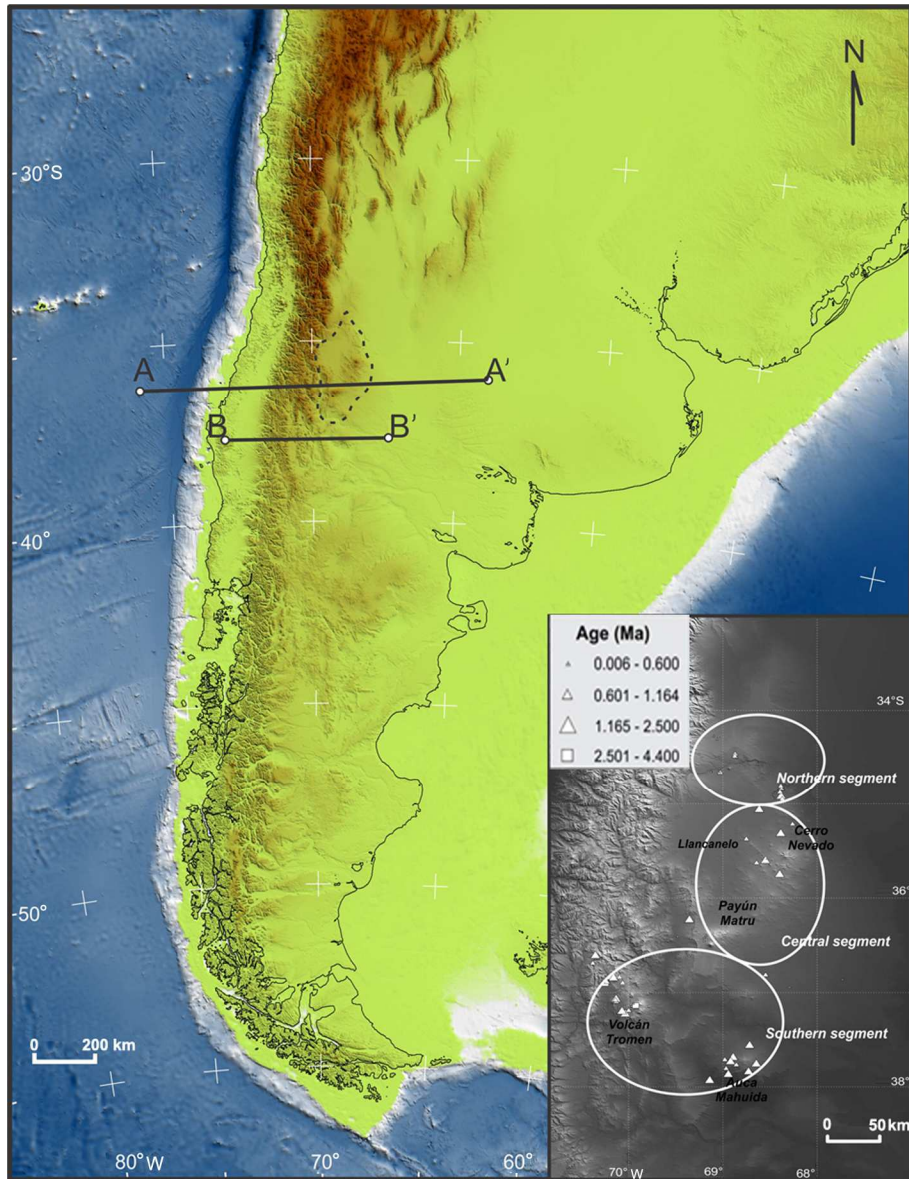
Table 2 Volcanic volume calculated based on the topography and the age intervals.

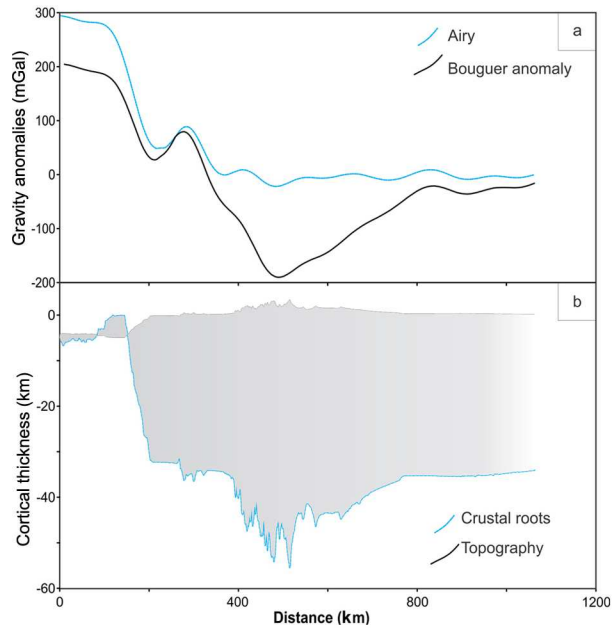
Age interval (My)	Area (km²)	Volume (km³)
0.0 – 0.6	3035.4	117.40
0.6 – 1.165	4049.8	418.28
1.165 – 2.5	19,603.9	933.48
Total	26,689	1469

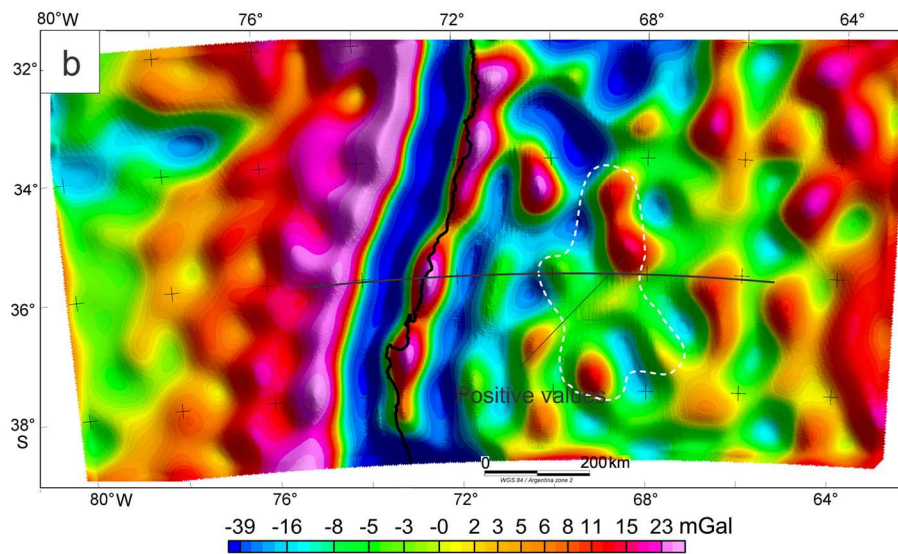
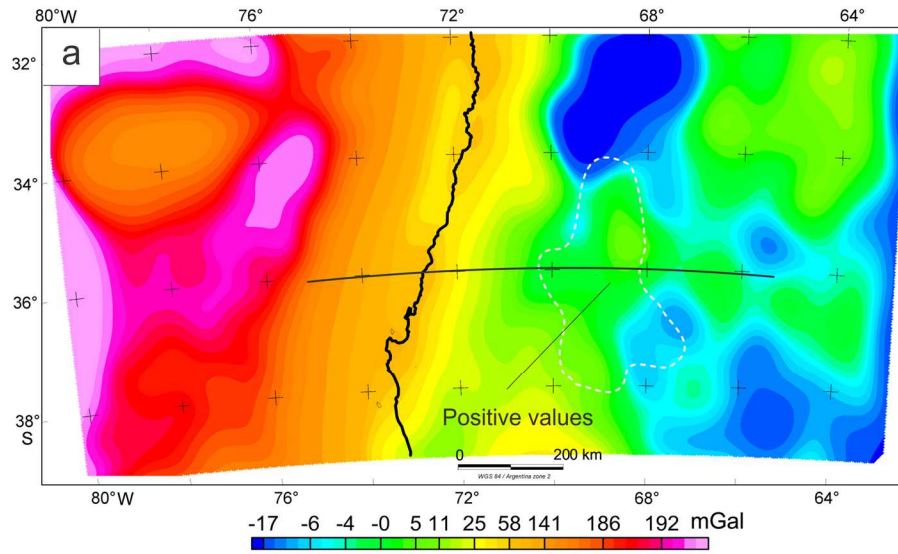
Table 3 Results of the extrusive vs. intrusive volumes of volcanic material.

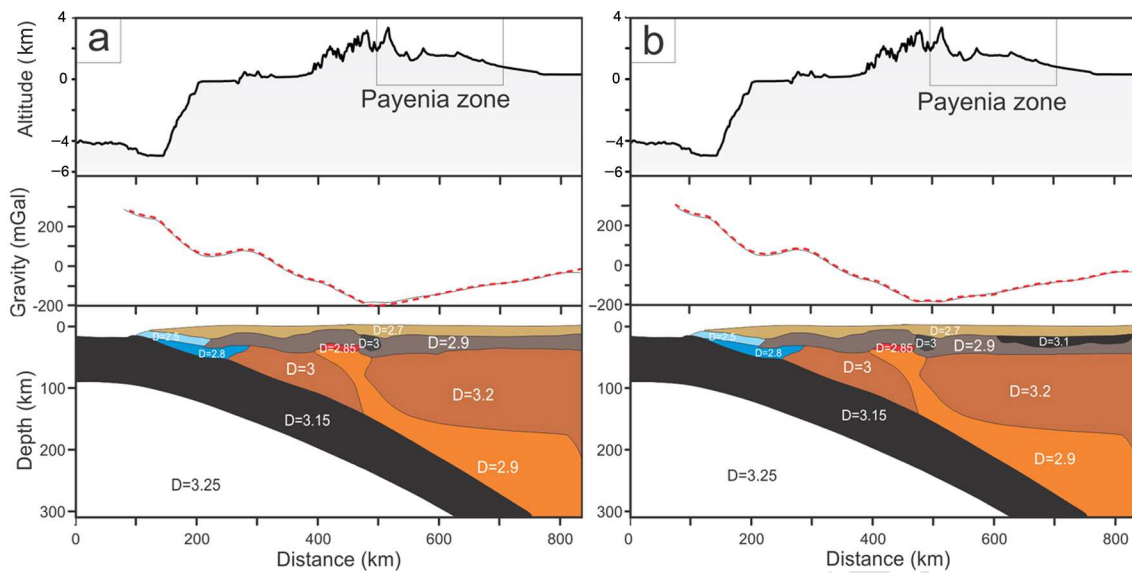
Surface (km ²)	Eruptive volume (km ³)	Relation		Thicknes s (km)	Intrusive volume (km ³)	Thicknes s (km)	Intrusive volume (km ³)	Thicknes s (km)
		16:1	5:1					
		Intrusive volume (km ³)						
40,660 ^a	9600	153,619	3.78	48,006	1.18	28,803	0.71	
39,638 ^b	8400	134,192	3.38	41,935	1.06	25,161	0.64	

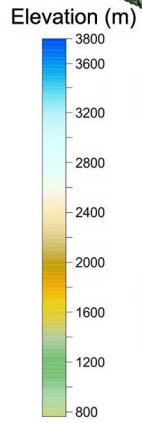
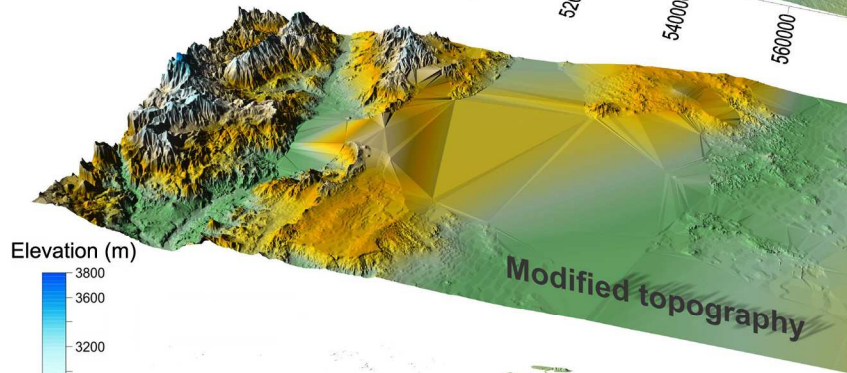
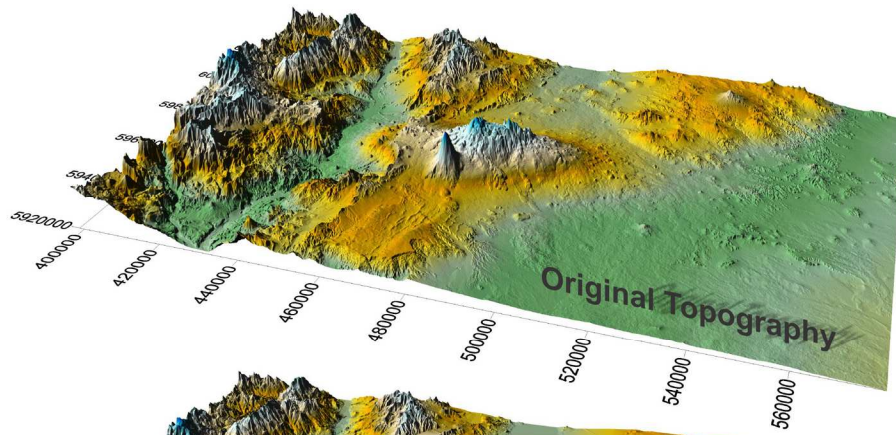
^aThis work; ^bRamos and Folguera (2011)

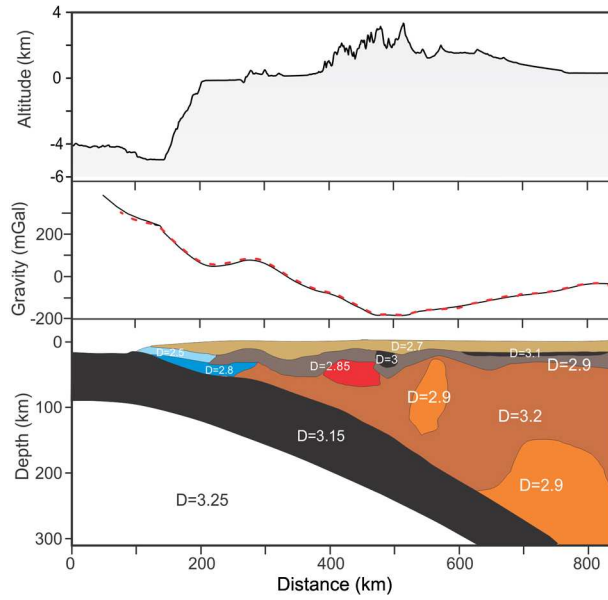


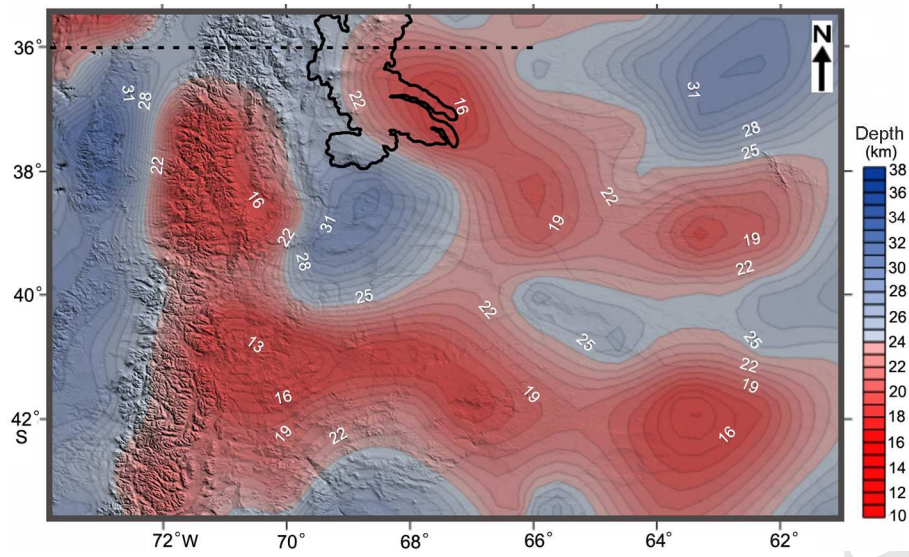












Payenia Quaternary flood basalts (Southern Mendoza, Argentina): Geophysical constraints on their volume

Mauro G. Spagnuolo^{a,*}, Darío L. Orts^b, Mario Gimenez^c, Andres Folguera^a, Victor A. Ramos^a

^a *Instituto de Estudios Andinos Don Pablo Groeber (I DEAN), UBA-CONICET*

^b *Instituto de Investigación en Paleobiología y Geología, Universidad Nacional de Río Negro – CONICET*

^c *Instituto Geofísico y Sismológico Ing. Volponi, Universidad Nacional de San Juan. CONICET*

Corresponding Author: Intendente Güiraldes 2160. Ciudad Universitaria - Pabellón II. C1428EGA – CABA, Argentina

Tel. (+54 +11) 4576-3400

E-mail address: mgspag@gmail.com (Mauro G. Spagnuolo)

Highlights

- We model different possible subsurface density model for Payenia.
- We examine gravity data to evaluate different models.
- We calculated the volume of volcanic material for Payenia region.
- We conjugate different lines of evidences to explain the density models.